Hematol Oncol Stem Cell Ther xxx (xxxx) xxx

Available at www.sciencedirect.com

ScienceDirect

journal homepage: www.elsevier.com/locate/hemonc

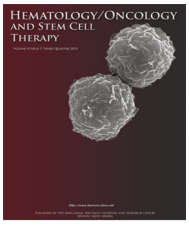

LETTER TO EDITOR

# Absence of FGFR3—TACC3 rearrangement in hematological malignancies with numerical chromosomal alteration

C. Banella [a,b], M. Ginevrino [c,d], G. Catalano [a,b], E. Fabiani [b], G. Falconi [b], M. Divona [e], P. Curzi [e], P. Panetta [e], M.T. Voso [a,b], N.I. Noguera [a,b,*]

[a] *Neuro-oncohematology Unit, IRCCS Santa Lucia Foundation, Rome, Italy*
[b] *Department of Biomedicine and Prevention, University of Rome Tor Vergata, Rome, Italy*
[c] *Neurogenetics Unit, IRCCS Santa Lucia Foundation, Rome, Italy*
[d] *Deparment of Molecular Medicine, University of Pavia, Pavia, Italy*
[e] *Policlinico Tor Vergata, Rome, Italy*

Received 10 December 2019; received in revised form 29 January 2020; accepted 7 February 2020

**KEYWORDS**
Acute myeloid leukemia;
Aneuploidy;
FGFR3—TACC3;
Glioblastoma;
Myelodysplastic syndromes

**Abstract**
FGFR—TACC, found in different tumor types, is characterized by the fusion of a member of fibroblast grown factor receptor (FGFR) tyrosine kinase (TK) family to a member of the transforming acidic coiled-coil (TACC) proteins. Because chromosome numerical alterations, hallmarks of FGFR—TACC fusions are present in many hematological disorders and there are no data on the prevalence, we studied a series of patients with acute myeloid leukemia and myelodysplastic syndrome who presented numerical alterations using cytogenetic traditional analysis. None of the analyzed samples showed *FGFR3—TACC3* gene fusion, so screening for this mutation at diagnosis is not recommended.


*Abbreviations*: GBM, glioblastoma multiforme; AML, acute myeloid leukemia; MDS, myelodysplastic syndromes; CML, chronic myeloid leukemia; FGFR, fibroblast grown factor receptor; TACC, transforming acidic coiled-coil; NGS, next-generation sequencing; BM, bone marrow

* Corresponding author at: Department of Biomedicine and Prevention, University of Rome, Tor Vergata, 00133 Rome, Italy.
*E-mail address:* n.noguera@hsantalucia.it (N.I. Noguera).

*To the Editor:*

Glioblastoma is the most aggressive among brain cancers with a median survival of 12—15 months and with less than 3—5% survival rate at 5 years [1]. Recently, a new molecular abnormality has been identified in 3% of a subset of human glioblastoma multiforme (GBM), characterized by the fusion

https://doi.org/10.1016/j.hemonc.2020.02.005
1658-3876/

Please cite this article as: C. Banella, M. Ginevrino, G. Catalano et al., Absence of FGFR3–TACC3 rearrangement in hematological malignancies with numerical chromosomal alteration, Hematol Oncol Stem Cell Ther, https://doi.org/10.1016/j.hemonc.2020.02.005

of a member of fibroblast grown factor receptor (FGFR) tyrosine kinase (TK) family to a member of the transforming acidic coiled-coil (TACC) proteins [2,3] FGFR—TACC fusion transcripts, which have been found in different tumor types [4], confer a phenotype combining growth-promoting effects with aneuploidy through a yet unclear mechanism. FGFR—TACC fusion proteins feature a constitutively active TK and are considered tumor-initiating events, and are highly sensitive to specific tyrosine kinase inhibitors [3,5—7].

FGFR signaling is important for central nervous system development and contributes to regulate cell proliferation, survival, and cytoskeletal regulation. Molecular anomalies of FGFR have been implicated in tumor development and progression [8].

TACC proteins are essential for the stabilization of kinetochore fibers and the mitotic spindle driving the chromosomal separation during prometaphase.

In 4853 tumor samples analyzed by Helsten et al. [9], FGFR alterations were found in about 7% of cases encompassing 47 histological types (urothelial, 31.7%; breast, 17.4%; endometrial, 11.3%; endometrial/ovarian carcinomas, 8.1%). Only 28 of these exhibited *FGFR* gene fusions, and 14 samples had *FGFR3—TACC3* fusions [9]. FGFR—TACCs activate the phosphoinositide 3-kinase (PI3K)/AKT/mammalian target of rapamycin (mTOR) pathway and cause alterations of the cell cycle control genes as CDK4, CDK2, and CCNE1 [10]. Currently, several clinical trials are in progress targeting the FGFR pathway in solid and hematological malignancies.

AML is a heterogeneous group of hematological neoplasms. Cytogenetic and molecular profiling allows disease stratification and has a significant impact on therapeutic choices. Because chromosome numerical alterations, hallmarks of FGFR—TACC fusions, are present in many hematological disorders and there are no available data on the prevalence [9], we studied a series of patients with acute myeloid leukemia (AML) and myelodysplastic syndrome (MDS) who presented numerical alterations by cytogenetic traditional analysis.

FGFR3—TACC3 fusion is difficult to identify using traditional cytogenetic banding analysis, and identification by fluorescence in situ hybridization (FISH) is technically challenging because of the proximity of the two parental genes. The most common method used to identify FGFR3—TACC3 is reverse transcription polymerase chain reaction (RT—PCR) in addition to next-generation sequencing (NGS) targeted to FGFR.

Because FGFR3—TACC3 mutation is associated with numerical abnormalities in different cancers, for this study we selected a cohort of 40 AML, 11 MDS, and two chronic myeloid leukemia (CML) patients who had numerical chromosome alterations at conventional karyotype analysis, from 1200 patients studied at diagnosis at the Department of Biomedicine and Prevention, University of Rome Tor Vergata, Rome, Italy, between 2014 and 2018. Written informed consent was obtained from all patients according to institutional guidelines and the Declaration of Helsinki. The study had been approved by the institutional ethical commitment of Policlinico Tor Vergata, Rome.

Conventional karyotyping was performed and reported according to the International System for Human Cytogenetic Nomenclature. For molecular diagnostic studies, total RNA was extracted from bone marrow (BM) mononuclear cells separated by Ficoll—Hypaque [11].

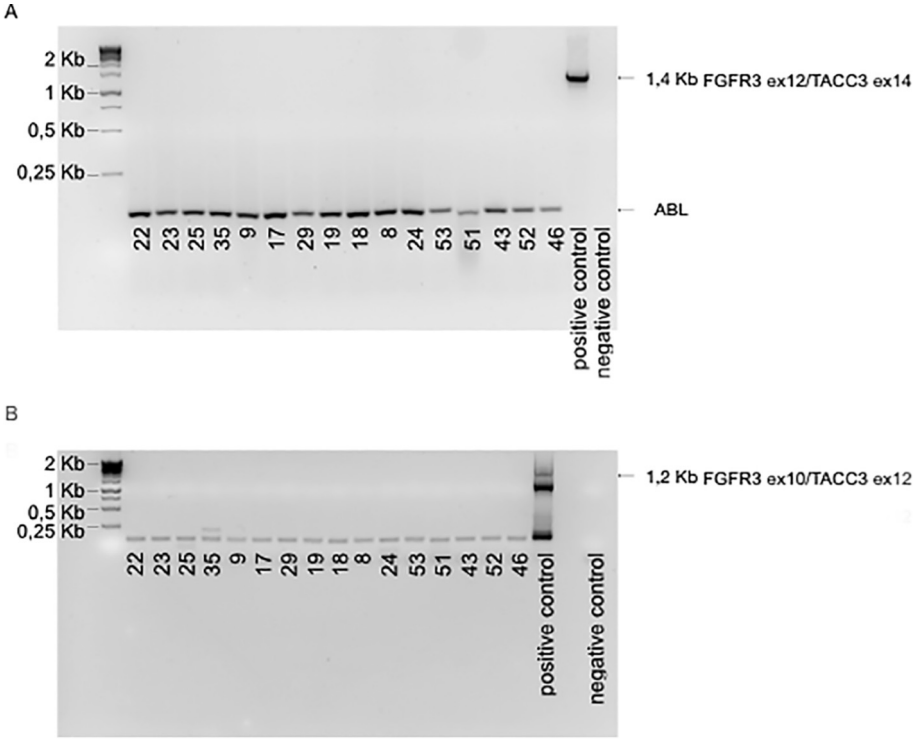


**Fig. 1** Representative results of FGFR3ex12_TACC3ex14 PCR (a) and FGFR3ex10_TACC3ex12 nested PCR (b) of line 11 AML and 6 MDS samples are shown. AML = acute myeloid leukemia; MDS = myelodysplastic syndrome; PCR = polymerase chain reaction.

Please cite this article as: C. Banella, M. Ginevrino, G. Catalano et al., Absence of FGFR3–TACC3 rearrangement in hematological malignancies with numerical chromosomal alteration, Hematol Oncol Stem Cell Ther, https://doi.org/10.1016/j.hemonc.2020.02.005

**Table 1** Molecular and cytogenetic characterization of sample patients.

| Code number | Disease | Karyotype | Molecular alteration |
|---|---|---|---|
| 1 | AML | 47,XY,+8[20] | Not available |
| 2 | AML | 47,XY,+8[20] | AML1/ETO neg; CBFb/MYH11 neg; DEK/CAN neg; BCR/ABL neg; FLT3 (ITD) pos; NPM1 neg |
| 3 | AML | 48,XY,+4,dup(5)(p15.1p13),+8 | AML1/ETO neg; CBFb/MYH11 neg; DEK/CAN neg; BCR/ABL neg; FLT3 (ITD) neg; NPM1 neg |
| 4 | AML | 47,XY,+14,+21,der(21;22)(q11;q11)[5]/47,XY,+14[3]/46,XY[7] | AML1/ETO neg; CBFb/MYH11 neg; DEK/CAN neg; BCR/ABL neg; FLT3 (ITD) neg; NPM1 neg |
| 5 | AML | 50,XY,+1,+6,der(7)(p12),+8,der(11)(p15),+der(11)(p15) | AML1/ETO neg; CBFb/MYH11 neg; DEK/CAN neg; BCR/ABL neg; FLT3 (ITD) neg; NPM1 neg |
| 6 | AML | 47,XY,+8[14]/46,XX[1] | AML1/ETO neg; CBFb/MYH11 neg; DEK/CAN neg; BCR/ABL neg; FLT3 (ITD) neg; NPM1 neg |
| 7 | AML | 43,XY,+del5q31,−6,−10,−11,−14,+M[9]/46,XY[4] | AML1/ETO neg; CBFb/MYH11 neg; DEK/CAN neg; BCR/ABL neg; FLT3 (ITD) neg; NPM1 neg |
| 8 | AML | 50,XY,+4,+20,+22,+M | AML1/ETO neg; CBFb/MYH11 neg; DEK/CAN neg; BCR/ABL neg; FLT3 (ITD) neg; NPM1 neg |
| 9 | AML | 50,XX,+4,+6,+8,inv(16)(p13q22)[18]/46,XX[2] | Not available |
| 10 | AML | 47,XY,del(3q),+8[18]/46,XY[2] | AML1/ETO neg; CBFb/MYH11 neg; DEK/CAN neg; BCR/ABL neg; FLT3 (ITD) neg; NPM1 neg |
| 11 | AML | 47,XY,+8[20] | not available |
| 12 | AML | 47,XY,del(5)(q13q33),+8[7]/46,XY[3] | AML1/ETO neg; CBFb/MYH11 neg; DEK/CAN neg; BCR/ABL neg; FLT3 (ITD) neg; NPM1 neg |
| 13 | AML | 47,XX,+5[14]/46,XX[6] | AML1/ETO neg; CBFb/MYH11 neg; DEK/CAN neg; BCR/ABL neg; FLT3 (ITD) neg; NPM1 neg |
| 14 | AML | 47,XY,+13[8]/46,XY,+M[2]/46,XY[10] | AML1/ETO neg; CBFb/MYH11 neg; DEK/CAN neg; BCR/ABL neg; FLT3 (ITD) neg; NPM1 neg |
| 15 | AML | 47,XY, +8[8]/46,XY [2] | Not available |
| 16 | AML | 45,XX,−7 | AML1/ETO neg; CBFb/MYH11 neg; DEK/CAN neg; BCR/ABL neg; FLT3 (ITD) neg; NPM1 neg |
| 17 | AML | 48,XX,+8,+22,inv(16) | AML1/ETO neg; CBFb/MYH11 pos type A; DEK/CAN neg; BCR/ABL neg; FLT3 (ITD) neg; NPM1 neg |
| 18 | AML | 64−71 chromosomes | AML1/ETO neg; CBFb/MYH11 neg; DEK/CAN neg; BCR/ABL neg; FLT3 (ITD) neg; NPM1 neg |
| 19 | AML | 45,XX,−5,der(7)t(7;?),−13,der(16)t(16;?),−20 | AML1/ETO neg; CBFb/MYH11 neg; DEK/CAN neg; BCR/ABL neg; FLT3 (ITD) neg; NPM1 neg |
| 20 | AML | 48,XX,+8,inv(16),+22 | AML1/ETO neg; CBFb/MYH11 pos; DEK/CAN neg; BCR/ABL neg; FLT3 (ITD) neg; NPM1 neg |
| 21 | AML | 45,XY,der(3)t(3;?),−7 | Not available |
| 22 | AML | 45,XY,−10,der(18)t(10;18) | AML1/ETO neg; CBFb/MYH11 neg; DEK/CAN neg; BCR/ABL neg; FLT3 (ITD) neg; NPM1 neg |
| 23 | AML | 47,XX,+8 | AML1/ETO neg; CBFb/MYH11 neg; DEK/CAN neg; BCR/ABL neg; FLT3 (ITD) neg; NPM1 neg |
| 24 | AML | 47,XX,del(4q),der(5)t(5;?),del(9),+11 | AML1/ETO neg; CBFb/MYH11 neg; DEK/CAN neg; BCR/ABL neg; FLT3 (ITD) neg; NPM1 neg |
| 26 | AML | 45,X0 | AML1/ETO neg; CBFb/MYH11 neg; DEK/CAN neg; BCR/ABL neg; FLT3 (ITD) neg; NPM1 neg |
| 27 | AML | 48,XX,del(5q),del(6q),del(7q),del(11q),+2mar | AML1/ETO neg; CBFb/MYH11 pos; DEK/CAN neg; BCR/ABL neg; FLT3 (ITD) neg; NPM1 neg |
| 28 | AML | 47,XX,+8 | AML1/ETO neg; CBFb/MYH11 neg; DEK/CAN neg; BCR/ABL neg; FLT3 (ITD) neg; NPM1 neg |
| 29 | AML | 48,XX,del(5q),−7,add(11p),−19,−21,+5mar | AML1/ETO neg; CBFb/MYH11 pos; DEK/CAN neg; BCR/ABL neg; FLT3 (ITD) neg; NPM1 neg |
| 30 | AML | 46,XY,−5,del(13q),der(17)t(17;?) | AML1/ETO neg; CBFb/MYH11 neg; DEK/CAN neg; BCR/ABL neg; FLT3 (ITD) neg; NPM1 neg |
| 31 | AML | 45,XY,del(5q),del(6p),−7 | AML1/ETO neg; CBFb/MYH11 neg; DEK/CAN neg; BCR/ABL neg; FLT3 (ITD) neg; NPM1 neg |

Please cite this article as: C. Banella, M. Ginevrino, G. Catalano et al., Absence of FGFR3–TACC3 rearrangement in hematological malignancies with numerical chromosomal alteration, Hematol Oncol Stem Cell Ther, https://doi.org/10.1016/j.hemonc.2020.02.005

**Table 1** (continued)

| Code number | Disease | Karyotype | Molecular alteration |
|---|---|---|---|
| 32 | AML | 45,XX,−7 | AML1/ETO neg; CBFb/MYH11 neg; DEK/CAN neg; BCR/ABL neg; FLT3 (ITD) neg; NPM1 neg |
| 33 | AML | 45,XY,del(1p),del(4q),−5,der(11)t(11;?),der(12)t (12;?),−16,der(16)t(16;?),+mar | AML1/ETO neg; CBFb/MYH11 neg; DEK/CAN neg; BCR/ABL neg; FLT3 (ITD) neg; NPM1 neg |
| 34 | AML | 45,XX,t(1;4),del(5q),−7 | AML1/ETO neg; CBFb/MYH11 neg; DEK/CAN neg; BCR/ABL neg; FLT3 (ITD) neg; NPM1 neg |
| 36 | AML | 46,XY,del(5q),−7,+mar | AML1/ETO neg; CBFb/MYH11 neg; DEK/CAN neg; BCR/ABL neg; FLT3 (ITD) neg; NPM1 neg |
| 37 | AML | 45,XX,+1,−4,del(5q),+8,−13,−15,−19,−20,−21,−22, +4mar | AML1/ETO neg; CBFb/MYH11 neg; DEK/CAN neg; BCR/ABL neg; FLT3 (ITD) neg; NPM1 neg |
| 38 | AML | 43,XY,del(5q),−7,−12,−13,+6,−17,−18,+20,+2mar | AML1/ETO neg; CBFb/MYH11 neg; DEK/CAN neg; BCR/ABL neg; FLT3 (ITD) neg; NPM1 neg |
| 39 | AML | 47,XY,+8 | AML1/ETO neg; CBFb/MYH11 neg; DEK/CAN neg; BCR/ABL neg; FLT3 (ITD) neg; NPM1 pos |
| 40 | AML | 45,XY,−7 | AML1/ETO neg; CBFb/MYH11 neg; DEK/CAN neg; BCR/ABL neg; FLT3 (ITD) neg; NPM1 neg |
| 41 | AML | 46,XY,del(1q),−5,del(7q),der(12)t(12;?),add(13p),del (17p). + mar | Not available |
| 42 | AML | 45,XY,−5.der(15)t(15;?),−16,+mar | AML1/ETO neg; CBFb/MYH11 neg; DEK/CAN neg; BCR/ABL neg; FLT3 (ITD) neg; NPM1 neg |
| | CML | 45,XY,+der(1),−2,del(5q),−13,−19,+3mar | not available |
| | CML | 45,XX,−7,t(9;22) | AML1/ETO neg; CBFb/MYH11 neg; DEK/CAN neg; BCR/ABL pos; FLT3 (ITD) neg; NPM1 neg |
| 43 | MDS | 45,XX,der(1)t(1;17)(p11;q11),der(5)t(5q;?),−17 | ASXL1 L775*fs (10,8%); CSF3R neg; DNMT3A neg; EZH2 E51*(12,5%); IDH1 R132C(7%); IDH2 R140Q(1.3%); PTPN11 neg; RUNX1 H242Tfs* (12,2%); SETBP1 neg; SF3B1 neg; TET2 neg; P53 neg; ZRSF2 neg |
| 44 | MDS | 46,XX in 4 metaphases, 45XX de(1)(p31\ p12), der(5)t (5;6) (q13;p25), del (13)(q13 q14) in 19 metaphases | ASXL1 neg; CSF3R neg; DNMT3A N501S (46,1%); EZH2 neg; IDH1 neg; IDH2 neg; PTPN11 neg; RUNX1 neg; SETBP1 I404V (50%); SF3B1 neg; TET2 P333L(50,2%); P53 H115Afs* (3,2%) e splice c.559 + 1G > A (2,2%); ZRSF2 neg |
| 45 | MDS | 40,X,−Y,+der(3), del(5)(q13q33),der(7),−9,−14,der(17) t(9;17)(p12;p11),der(22)add(p11) | ASXL1 neg; CSF3R Q749*(2,4%) e Q739*(6,1%); DNMT3A neg; EZH2 neg; IDH1 neg; IDH2 neg; PTPN11 T73I(1,2%); RUNX1 neg; SETBP1 neg; SF3B1 neg; TET2 neg; P53 neg; ZRSF2 neg |
| 46 | MDS | 46,XX,del(5)(q13q33),i(7)(q10),der(17)t(12;17)(p13; p21)t(17;20)(q11q13),ish der(17)(TP53−,D17Z1 + )t (12;17)(TP53+,D17Z1 + )−;TP53−,D17Z1 + ) su 21 metaphases/46,XX su 4 metaphases | ASXL1 neg; CSF3R neg; DNMT3A neg; EZH2 neg; IDH1 neg; IDH2 neg; PTPN11 neg; RUNX1 L56S(48,2%); SETBP1neg; SF3B1 neg; TET2 neg; P53 C242Y (45%) e I162N(46,8%); ZRSF2 neg |
| 47 | MDS | Presence of a single metaphase with a normal male karyotype and of 3 altered lines: one characterized by monosomy of chromosome 7 (2 metaphases); one characterized by terminal deletion of the short arm of a chromosome 12 (5 metaphases) | ASXL1 neg; CSF3R neg; DNMT3A neg; EZH2 neg; IDH1 neg; IDH2 neg; PTPN11 neg; RUNX1 L56S(48,3%); SETBP1neg; SF3B1 neg; TET2 neg; P53 S127F (92.6%); ZRSF2 neg |
| 48 | MDS | 40−42,XX,del(3)(p11),−5,−11,−12,−13,−14,add(14) (q24),−18,−20,+3mar[cp4]/46,XX[6] | ASXL1 E1102D(51,5%) CSF3R neg; DNMT3A neg; EZH2 neg; IDH1 neg; IDH2 neg; PTPN11 neg; RUNX1 neg; SETBP1 P301L(1,1%); SF3B1 neg; TET2 neg; P53 S241Y (70,4%); ZRSF2 neg |

Please cite this article as: C. Banella, M. Ginevrino, G. Catalano et al., Absence of FGFR3–TACC3 rearrangement in hematological malignancies with numerical chromosomal alteration, Hematol Oncol Stem Cell Ther, https://doi.org/10.1016/j.hemonc.2020.02.005

**Table 1** (continued)

| Code number | Disease | Karyotype | Molecular alteration |
|---|---|---|---|
| 49 | MDS | 41—46,XY,del(4)(q21),del(5)(q14),del(7)(q22),—11,der(12)t(12;?),—13,+21,+mar su 18 cell./ 46,XY su 2 cell | ASXL1 neg; CSF3R neg; DNMT3A neg; EZH2 neg; IDH1 neg; IDH2 neg; PTPN11 neg; RUNX1 p.Tyr349Alafs*(25,6%); SETBP1neg; SF3B1 neg; TET2 neg; P53 p.Phe338Serfs*7(2,2%) e p.Tyr220Cys(32,6%) e p.Pro177Ser(30,3%); ZRSF2 neg |
| 50 | MDS | 45,XY,der(5)t(5;?)(q13;?),—7,add(8)(p21),del(12)(p11,2) | ASXL1 neg; CSF3R neg; DNMT3A Q231*(3,6%); EZH2 neg; IDH1 neg; IDH2 neg; PTPN11 neg; RUNX1 neg; SETBP1neg; SF3B1 neg; TET2 neg; P53 R306* (6,9%); ZRSF2 neg |
| 51 | MDS | 46,XY[3/6] | ASXL1 neg; CSF3R neg; DNMT3A neg; EZH2 neg; IDH1 neg; IDH2 neg; PTPN11 neg; RUNX1 neg; SETBP1neg; SF3B1 (K700E(2,6%); TET2 neg; P53 C277Y (19,8%); ZRSF2 neg |
| 52 | MDS | 42—45,XY,del(1p),del(6q),—7,—8,add(10p),—17,?add(18p,del(20q),+mar1,+mar2 | ASXL1 I981*fs (41,5%) e S1422T (1,1%); CSF3R neg; DNMT3A R882H (45.6%); EZH2 neg; IDH1 neg; IDH2 neg; PTPN11 neg; RUNX1 neg; SETBP1 D868N (44.2%); SF3B1 neg; TET2 neg; P53 neg; ZRSF2 neg |
| 53 | MDS | 45,X,+X,—Y,del(3)(p2?1),del(5)(q14q34),—7,add(12)(p?12),—15,der(17)t(Y;17)(q11;p?11),+mar[19]/47,XXYc[1] | ASXL1p.Ala716Glufs*7(19,2%); CSF3R neg; DNMT3A p.Glu30Ala(52,4%); EZH2 neg; IDH1 neg; IDH2 neg; PTPN11 neg; RUNX1 neg; SETBP1 neg; SF3B1 neg; TET2 p.Gln622*(3,8%); P53 neg; ZRSF2 neg |

AML = acute myeloid leukemia; CML = chronic myeloid leukemia; MDS = myelodysplastic syndrome.

Samples were characterized for the presence of *BCR—ABL*, *PML—RARA*, *CBFB—MHY11*, *RUNX1—RUNX1T1*, and *DEK—CAN* fusion genes, and for NPM1 and FLT3-internal tandem duplication (ITD) mutations using methods reported elsewhere [12,13]. MDS samples were characterized by ultra-deep NGS, using the commercial Myeloid Solution produced by SOPHiA GENETICS (Saint-Sulpice, Switzerland) on a HiSeq sequencing platform (Illumina, San Diego, CA, USA).

Total RNA was extracted from frozen blasts using Eurogold Trifast (Euroclone) according to the manufacturer's instructions. Briefly, 100 ng of total RNA were retro- transcribed with the Maxima First Strand cDNA Synthesis Kit (Thermo Scientific) or SuperScript II (Invitrogen). RT—PCR was performed using AccuPrime Taq DNA Polymerase (Invitrogen).

The primer pairs used for the FGFR3—TACC3 fusion screening were [14]: FGFR3ex12-FW: 5′-CGTGAAGATGCT GAAAGACGATG-3 and TACC3ex14-RV: 5′-AAACGCTTGAA GAGGTCGGAG; amplification conditions were as follows: 95 °C for 10 minutes (95 °C for 15 seconds/61 °C for 30 seconds/68 °C for 1 minute and 40 seconds) for 35 cycles, 72 °C for 5 minutes.

None of the analyzed samples showed *FGFR3—TACC3* gene fusion. To confirm the results, we designed a new primer pair and performed a nested PCR to reduce nonspecific binding in products because of the amplification of unexpected primer binding sites (Fig. 1). Data of molecular and cytogenetic analysis are reported in Table 1.

Primer pairs used for the FGFR3—TACC3 nested PCR were: FGFR3 ex10-FW: 5′-CTGAGATGGAGATGATGAAGATG-3′ and TACC3 ex12-RV: 5′-ATGGAGTTCAGATCTGTGGTAAG; amplification conditions were 95 °C for 10 minutes (95 °C for 15 seconds/61 °C for 30 seconds/68 °C for 1 minute and 40 seconds) for 35 cycles, 72 °C for 5 minutes.

A plasmid (pLOC FGFR3—TACC3) generously donated by Professor Antonio Iavarone was used as positive control.

Our data confirm the rarity of FGFR3—TACC3 rearrangement also in AML and myelodysplasia. Despite the limited number of samples, screening for this mutation at diagnosis is not recommended.

## Acknowledgements

This work was supported by AIRC 5x1000 call ''Metastatic disease: the key unmet need in oncology" to MYNERVA project, #21267 (MYeloid Neoplasms Research Venture Airc, a detailed description of the MYNERVA project is available at http://www.progettoagimm.it.) and by PRIN 2017WXR7ZT_004.

## Authors' contributions

CB: study design, performance and analysis of experiments, writing of the manuscript; MG: study design; GC: data analysis, writing of the manuscript; EF, GF, MD: characterization and collection of samples from AML and MDS patients; PC and PP: cytogenetic characterization; MTV: critical review of the manuscript, and amended the final report; NIN: study design, writing of the manuscript, and supervision of research.

Please cite this article as: C. Banella, M. Ginevrino, G. Catalano et al., Absence of FGFR3–TACC3 rearrangement in hematological malignancies with numerical chromosomal alteration, Hematol Oncol Stem Cell Ther, https://doi.org/10.1016/j.hemonc.2020.02.005

## Declaration of Competing Interest

The authors declare that they have no known competing financial interests or personal relationships that could have appeared to influence the work reported in this paper.

## References

[1] Wirsching H-G, Galanis E. Glioblastoma. San Diego: Elsevier; 2016. p. 381–97.
[2] Singh D, Chan JM, Zoppoli P, Niola F, Sullivan R, Castano A, et al. Transforming fusions of FGFR and TACC genes in human glioblastoma. Science 2012;337:1231–5.
[3] Lasorella A, Sanson M, Iavarone A. FGFR–TACC gene fusions in human glioma. Neuro Oncol 2017;19:475–83.
[4] Nelson KN, Meyer AN, Siari A, Campos AR, Motamedchaboki K, Donoghue DJ. Oncogenic gene fusion FGFR3–TACC3 is regulated by tyrosine phosphorylation. Mol Cancer Res 2016;14:458–69.
[5] Wang Z, Zhang C, Sun L, Liang J, Liu X, Li G, et al. FGFR3, as a receptor tyrosine kinase, is associated with differentiated biological functions and improved survival of glioma patients. Oncotarget 2016;7:84587–93.
[6] Tamura R, Yoshihara K, Saito T, Ishimura R, Martinez-Ledesma JE, Xin H, et al. Novel therapeutic strategy for cervical cancer harboring FGFR3–TACC3 fusions. Oncogenesis 2018;7:4.
[7] Chen CH, Liu YM, Pan SL, Liu YR, Liou JP, Yen Y. Trichlorobenzene-substituted azaaryl compounds as novel FGFR inhibitors exhibiting potent antitumor activity in bladder cancer cells in vitro and in vivo. Oncotarget 2016;7:26374–87.
[8] Haugsten EM, Wiedlocha A, Olsnes S, Weshe J. Roles of fibroblast growth factor receptors in carcinogenesis. Mol Cancer Res 2010;8:1439–52.
[9] Helsten T, Elkin S, Arthur E, Tomson BN, Carter J, Kurzrock R. The FGFR landscape in cancer: analysis of 4,853 tumors by next-generation sequencing. Clin Cancer Res 2016;22:259–67.
[10] Costa R, Carneiro BA, Taxter T, Tavora FA, Kalyan A, Pai SA, et al. FGFR3–TACC3 fusion in solid tumors: mini review. Oncotarget 2016;7:55929–38.
[11] Noguera NI, Piredda ML, Taulli R, Catalano G, Angelini G, Gaur G, et al. PML/RARa inhibits PTEN expression in hematopoietic cells by competing with PU.1 transcriptional activity. Oncotarget 2016;7:66386–97.
[12] Noguera NI, Ammatuna E, Zangrilli D, Lavorgna S, Divona M, Buccisano F, et al. Simultaneous detection of NPM1 and FLT3–ITD mutations by capillary electrophoresis in acute myeloid leukemia. Leukemia 2005;19. https://doi.org/10.1038/sj.leu.2403846.
[13] Calvo KL, Ojeda MJ, Ammatuna E, Lavorgna S, Ottone T, Targovnik HM, et al. Detection of the nucleophosmin gene mutations in acute myelogenous leukemia through RT–PCR and polyacrylamide gel electrophoresis. Eur J Haematol 2009;82:69–72.
[14] Di Stefano AL, Fucci A, Frattini V, Labussiere M, Mokhtari K, Zoppoli P, et al. Detection, characterization, and inhibition of FGFR–TACC fusions in IDH wild-type glioma. Clin Cancer Res 2015;21:3307–17.

Please cite this article as: C. Banella, M. Ginevrino, G. Catalano et al., Absence of FGFR3–TACC3 rearrangement in hematological malignancies with numerical chromosomal alteration, Hematol Oncol Stem Cell Ther, https://doi.org/10.1016/j.hemonc.2020.02.005